Modeling of giant ELM effects on impurity enrichment in DIII-D*

J. Hogan[1], M. Wade[1], D. Hillis [1], M. Schaffer [+], P. West [+]
[1] Oak Ridge National Laboratory, Oak Ridge, TN, USA
[+] General Atomics, San Diego, CA, USA

1. INTRODUCTION

The attractiveness of H-mode plasmas with large scale ("type I") ELMs in attaining steady-state thermonuclear conditions will depend, in part, on the relation between ELM benefits (efficient core impurity removal, especially of helium ash) and drawbacks (intense heat flux pulses). A better quantitative model for this trade-off is needed. The time-dependent B2-Eirene divertor transport code [1] is thus used to explore questions raised by DIII-D neon and argon injection and exhaust experiments [2]. In these experiments (lower single null divertor, ELM frequency f_{ELM}~ 50-60 Hz) plenum impurity enrichment was increased by inducing a D^+ scrape-off layer flow with midplane D_2 puffing, in comparison with results using divertor D_2 puffing and otherwise similar conditions [3]. While previous studies have emphasized the adequacy of attainable divertor enrichment with respect to detailed reactor designs (e.g., ITER), this is a fundamental problem for the applicability of the tokamak concept and a more detailed understanding is needed. However, since the divertor Thomson scattering pulse repetition frequency is 20 Hz and the plenum enrichment measurement is averaged over several ELM cycles, the fundamental processes which determine enrichment with giant ELMs cannot be directly measured at present. Thus, the modeling work is aimed at delineating the basic processes involved and suggesting directions for further diagnostic development.

2. B2-EIRENE ELM SIMULATION

A 19-species version of the B2-Eirene code prepared by D. Coster (IPP-Garching) is used for a time-dependent calculation of ELM behavior under conditions of the DIII-D puff and pump experiments. All ion species of D, C, Ne, and He are included. Neutral behavior is calculated with the implicitly coupled Eirene '93 code. The DIII-D magnetic geometry and sample D, D_2 particle tracks from Eirene are shown in Fig. 1. Divertor puffing in the simulations is done from the DIMEs port location (shown) and midplane puffing from the outboard equator. The D_2 puffing rate is 100 T l/s for each case (the level of the DIII-D injection/exhaust experiments). For these time-dependent ELM simulations, an effective albedo (95% recycling) is prescribed at the baffle entrance. The detailed cryo-pumping geometry shown here uses Eirene '97 and will be described in the future.

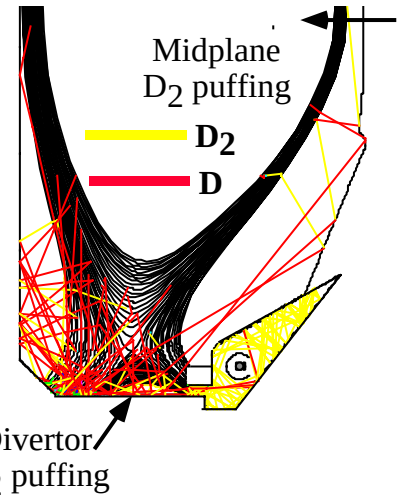

Fig. 1 DIII-D geometry for pumping using the lower baffle. Puffing locations are shown

This research was sponsored in part by the Office of Fusion Energy Sciences, U.S. Department of Energy, under contract DE-AC05-96OR22464 with Lockheed Martin Energy Research Corp. and DE-AC03-89ER51114.

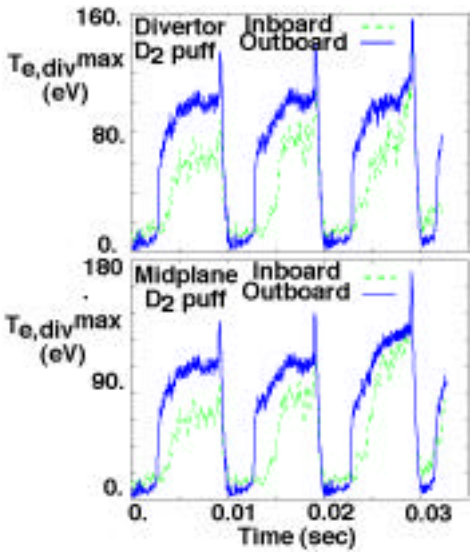

Fig. 2 Simulated time dependence (B2-EIRENE) of $T_{e,div}^{max}$ for outer (solid), and inner (dashed) strike points. Divertor (a, top) and midplane (b, bottom) D_2 puffing.

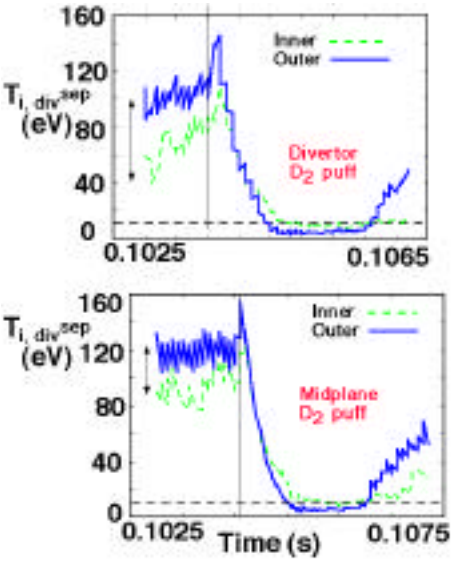

Fig. 3 Detail of one ELM event with divertor (a, top) and mid-plane (b, bottom) puffing showing $T_{i,div}^{sptrx}$ for outer (solid), and inner (dashed) strike points.

An ELM event is modeled by enhancing the electron and ion radial diffusivities by 5x during a 1000 μsec interval, with a prescribed frequency (100Hz in the case considered). Other aspects of the transport are unchanged and, after the ELM event, subsequent evolution is determined solely by the underlying radial transport and recycling. Figure 2 shows the resulting variation of $T_{e,div}$ during several cycles of ELM behavior for the simulation of D_2 puffing in the divertor (Fig. 2a) and midplane (Fig. 2b). For each ELM event in each of these cases there is a temperature crash just after ELM onset which produces $T_{e,div} < 5$ eV and a detached strike point. There follows a slow ($t_{recov} \sim 1/f_{ELM}$) recovery to the pre-ELM status. A slightly lower pre-crash $T_{e,div}$ is found for divertor puffing, while a stronger difference is observed for $T_{i,div}$ (Fig. 3a,b). In the divertor puffing case $T_{i,div}$ is 30% lower than for the midplane case, due to large CX losses from the localized gas puff in the divertor. If this reduction held over the whole ELM cycle it would imply that the concomitant reduction in the ion thermal force would be a more significant variable than induced SOL flow when comparing divertor and midplane puffing. However, as seen in Fig. 3b, the difference in $T_{i,div}$ for the two cases narrows with the onset of the crash, and thereafter, during the recovery phase $T_{i,div}$ is similar for both cases. Figures 2,3 thus show that the measurable background plasma conditions are similar in these impurity enrichment comparisons.

3. IMPURITY DYNAMICS

QuickTime (Macintosh) movies of impurity behavior during the ELM cycle of Figs. 2,3 have been prepared and are available via the Internet [4]. Figures 4-7 show snapshots from these sequences. Figure 4 shows the spatial distribution of D^+ ions near the DIII-D baffle entrance at the outer strike point during the detached phase of the ELM cycle, comparing divertor puffing (Fig. 4a) with midplane puffing (Fig.4b) cases. (Figure 4a also shows the grid which underlies Figs. 4-7). A pronounced local peak in D^+ density appears on the private flux side of the separatrix in the divertor puff case, leading to an instantaneous 50% increase in peak D^+ density. There are significant differences in the behavior of each of the impurity species, related to characteristic recycling processes. The neon ion density in the baffle region for the detached and recovery phases of the ELM cycle, in the case of midplane D_2 puffing, is shown if Figs. 5a,b. Since $T_{e,div}$ drops below the ionization potential for NeI at the outset of the ELM cycle (Fig. 2), the neon ion

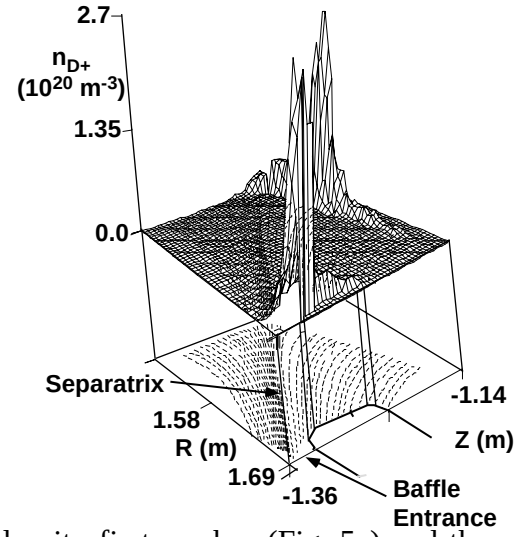

Fig. 4 (a) D^+ distributions in SOL near baffle for detached phase of ELM cycle for midplane D_2 puffing. The grid used for Figs 4-7 is also shown.

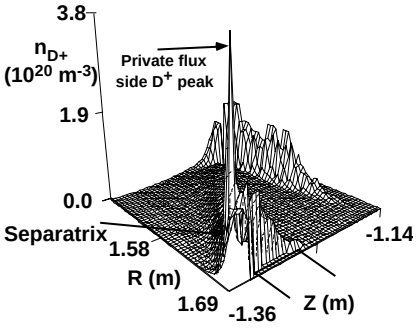

Fig. 4 (b) D^+ distributions in SOL near baffle for detached phase with divertor D_2 puffing.

density first crashes (Fig. 5a) and then, as $T_{e,div}$ rises, neon is re-ionized after having been dispersed throughout the region (Fig. 5b). During the ELM recovery phase there is considerable neon recycling from the front face of the baffle (Fig 5b), due to the prior dispersal of neon during the detached phase. The carbon density is peaked at or near the separatrix during the entire cycle (Fig. 6). For helium, there is a broad distribution but no evidence of baffle face recycling (Fig. 7). However, save for the local peak in deuterium recycling near the private region of the strike point in the divertor D_2 puff case, the dynamics are similar.

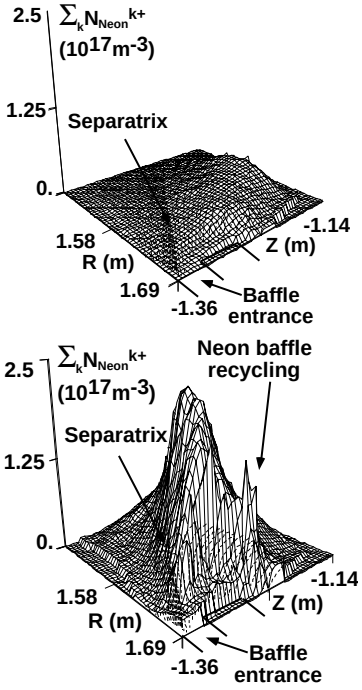

Fig. 5 (a,b) Neon ion distribution in SOL near baffle for the detached (a, top) and recovery (b, bottom) phases of the ELM cycle, for midplane D_2 puffing

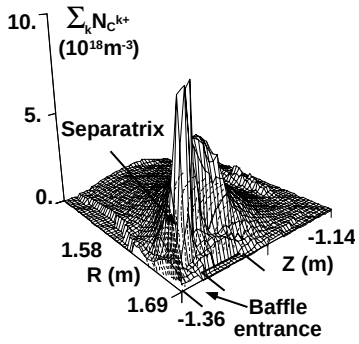

Fig. 6 C ion density near baffle for recovery phase with midplane D_2 pufing.

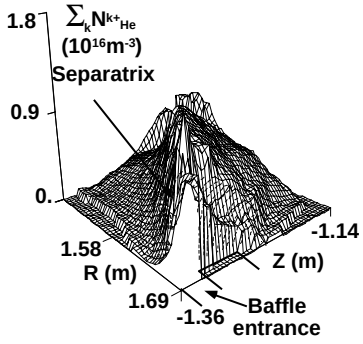

Fig. 7 He ion density near baffle for recovery phase (midplane D_2 puffing).

4. FLOW EFFECTS

The ELM detach-recovery sequence has important implications for impurity enrichment physics. Figure 8 shows the time dependence of neon and deuterium fluxes to the baffle during an ELM event for the divertor D_2 puffing case. As can be seen, there is a time shift between the peak D^+ flux and the neon flux. For conditions of high deuterium flux there is low neon flux, because the neon is not ionized. The neon flux to the baffle increases when the D flow subsides. Such effects are not extractable from a time averaged analysis. Figure 9 shows the D^+ and neon ion parallel flows in the SOL at the end of the ELM recovery phase. There is a significant induced D^+ flow, (Fig. 9a) and a resulting modification of the SOL impurity flow. A major effect of the induced SOL D^+ flow is to reduce

accumulation at the inner strike point, thus increasing the neon density at the outer strike point and resulting in increased concentration.

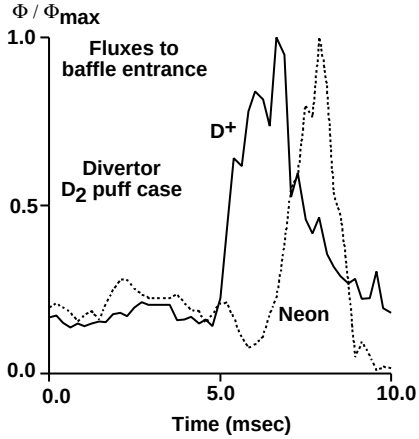

Fig. 8 Deuterium and neon fluxes to the baffle during an ELM event with divertor D_2 puffing

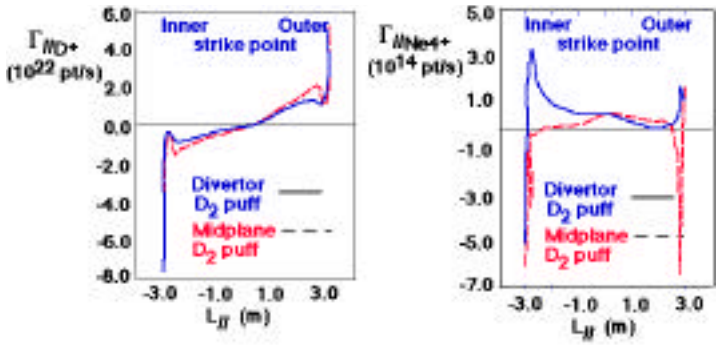

Fig. 9 Parallel D^+ and Ne^{4+} ion flows in the SOL for 100 T l /s D_2 puffing in the divertor (solid) and mid plane (dash)

5. CONCLUSIONS

For the (nominally) attached divertor conditions of the DIII-D impurity injection/exhaust experiments, B2-EIRENE modeling suggests a transient process with increased attachment just at the ELM event, followed by detachment at the outboard strike point (nearest the pump) just after an ELM, followed by a relatively long attached inter-ELM recovery period for $T_{e,div}$. The calculated time sequence of D^+ and neon ion fluxes to the baffle entrance during an ELM event are out of phase, and large deuterium fluxes precede large neon fluxes. This occurs because, during the detachment phase, $T_{e,div}$ is low enough that neon is poorly ionized near the baffle region, leading to dispersal. This subsequently leads to significant recycling of neon from the baffle face when T_e rises sufficiently for ionization. Behavior of other impurities differs: carbon (produced mainly by physical sputtering) is localized near the separatrix region, and no baffle source is found. Similarly for helium, no strong baffle recycling is observed since no dispersal results from the low $T_{e,div}$ phase. The recovery phase thus provides much of the observed enrichment, and during this quiescent phase there is a significant difference in SOL D^+ flow between divertor and midplane puffing cases. This leads to a pronounced effect in enhancing neon concentration near the baffle region. The balance between dispersal during detachment and concentration during the recovery phase remains to be determined experimentally. Absent this determination, cycle-averaged enrichment values may be ELM scenario-dependent and thus are not necessarily extrapolable to other devices.

ACKNOWLEDGEMENT

The B2-Eirene code is provided by the B2-Eirene development group: R. Schneider, D. Coster (IPP-Garching), D. Reiter (Univ. Duesseldorf), P. Boerner (FZ-Juelich)

REFERENCES

[1] R. Schneider et al, J. Nucl. Mater **196-8** (810) 1992
[2] M. Schaffer et al, J. Nucl. Mater., **241-3** (585) 1997
[3] M. Wade et al (Nucl Fusion, submitted)
[4] The Andrew File System: site /afs/nersc.gov/u/orn/u27725/B2-E